Dublin Institute of Technology
ARROW@DIT

Conference Papers | Dublin Energy Lab

2007-01-01

Modelling the Effect of Device Geometry on Concentration Ratios of Quantum Dot Solar Concentrators

Manus Kennedy
Dublin Institute of Technology, manus.kennedy@dit.ie

Sarah McCormack
Dublin Institute of Technology

John Doran
Dublin Institute of Technology

Brian Norton
Dublin Institute of Technology

Follow this and additional works at: http://arrow.dit.ie/dubencon2

 Part of the Engineering Commons

Recommended Citation

Kennedy, M., et al. (2007) Modelling the effect of device geometry on concentration ratios of quantum dot solar concentrators. *Proceedings of ISES 2007 Solar World Congress*, Beijing, China. DOI: 10.1007/978-3-540-75997-3_301

This Conference Paper is brought to you for free and open access by the Dublin Energy Lab at ARROW@DIT. It has been accepted for inclusion in Conference Papers by an authorized administrator of ARROW@DIT. For more information, please contact yvonne.desmond@dit.ie, arrow.admin@dit.ie, brian.widdis@dit.ie.

This work is licensed under a Creative Commons Attribution-Noncommercial-Share Alike 3.0 License

Modelling the effect of device geometry on concentration ratios of quantum dot solar concentrators

M. Kennedy*, S. J. McCormack, J. Doran, B. Norton
Dublin Energy Lab, Focas Institute, School of Physics, Dublin Institute of Technology, Dublin, Ireland.
*manus.kennedy@dit.ie

ABSTRACT

Quantum dot solar concentrators (QDSCs) are static, non-imaging concentrators which concentrate both direct and diffuse light. Using Monte-Carlo ray-trace modelling, concentration ratios (C) were predicted for QDSCs of different 2-D geometries. The optimum shape and size were determined, for given system parameters, by calculating the relative cost per unit power output. Devices with different 3-D geometry were also compared. The thickness of the plate was varied and devices with tapered thickness were modelled to investigate the effect on C.

1. INTRODUCTION

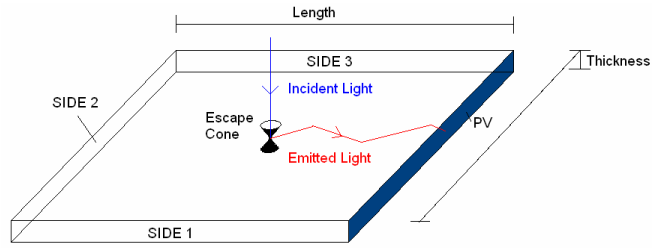

Fig. 1. QDSC consisting of a clear polymer plate doped with QDs, with PV cells attached to one side.

One approach to increasing the economic viability of photovoltaic (PV) cells for electricity generation is the concentration of incident solar energy. Luminescent solar concentrators (LSCs) [1,2] are static, non-imaging concentrators which do not require expensive solar tracking and concentrate both direct and diffuse light, a significant advantage in Northern European climates where >50% of total annual solar irradiation is diffuse. As incident insolation passes through a LSC device matrix, consisting of a flat polymer plate doped with a luminescent dye, it is absorbed by the dye. Longer wavelength light is emitted isotropically by the dye and is guided by total internal reflection (TIR) to one edge, where PV cells are attached (fig. 1). Mirrors can be placed adjacent and parallel to the rear surface and sides 1, 2 and 3 to reflect light that may be outside the angular range for TIR. A quantum dot solar concentrator (QDSC) [3] operates in the same way as an LSC, but employs quantum dots rather than a luminescent dye.

Current QDSCs [4] are fabricated using square plates of uniform thickness. This paper examines whether this is the optimum geometry, by calculating the relative cost per unit power output for varying device size and geometry type.

Geometric gain, G_{geom}, is defined as the concentrator plate top surface area, A_{conc}, divided by the total PV area, A_{pv} (eqn. 1). Geometries with a high G_{geom} are likely to have high concentration ratios, C. Higher C results in higher relative power output. If the cost of the concentrator plate is ignored then the geometry with the highest C would be the optimum. However, real devices will have a higher cost with increased G_{geom}. Considering both the relative power output and the relative cost of a device, the optimum 2-D geometry, for given system parameters, is determined in section 3.2. In section 3.3, it is investigated if devices with tapered thickness attain higher C than devices with uniform thickness.

$$G_{geom} = A_{conc} / A_{pv} \quad (1)$$

2. RAY TRACE MODEL AND INPUT PARAMETERS

Monte-Carlo ray-trace modelling is used to determine the optical efficiency (η_{opt}) of an LSC device [5,6,7,8,9]. η_{opt} is defined as the fraction of photons transmitted to the PV cell, compared to those incident on the concentrator top surface (eqn 2). C is given by eqn 3. To model a QDSC, a photon is traced through the QDSC until it is lost from the system or transmitted to the PV. The loss mechanisms included are escape-cone losses, matrix attenuation losses, quantum dot (QD) quantum efficiency (QE) losses, side mirror reflection losses, and initial top surface reflection losses. A wavelength independent matrix attenuation coefficient of $2cm^{-1}$ and a refractive index of 1.5 were assumed. The QD QE was assumed to be 100%, the external mirror reflection coefficient to be 0.94, and the incident light to be perpendicular to the top surface of the device.

$$\eta_{opt} = \frac{\text{total photons transmitted to PV}}{\text{total photons incident on top surface}} \quad (2)$$

$$C = \eta_{opt} G_{geom} \quad (3)$$

3. QDSC GEOMETRY

3.1 2-D Geometry Concentration Ratios

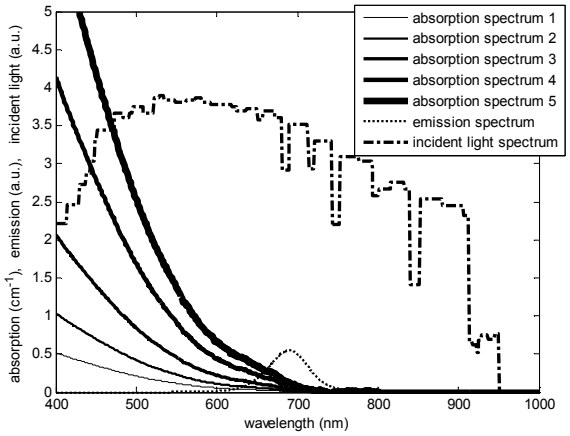

Fig. 2.Absorption spectrum 1 and the emission spectrum are measured spectra of CdSe QDs (CdS/CdZnS/Zn coating, fabricated at Utrecht University). Absorption spectra 2-5, corresponding to higher QD concentrations, are extrapolated from absorption spectrum 1. The incident light spectrum is the part of the AM 1.5 solar spectrum below 950nm.

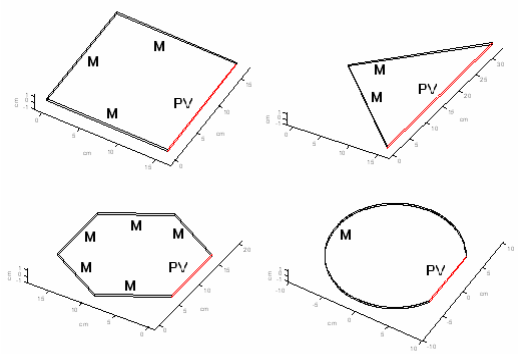

Fig. 3. Square, right angled triangular, hexagonal and circular (PV length=circle radius) devices, A_{conc}= 256cm^2. External mirrors (M) may be placed at the non PV sides, as shown here, or PV may be placed at all sides of the device.

Using QD absorption spectrum 5 and the input light spectrum shown in Fig. 2, C was calculated for varying A_{conc} using different geometries. Square, right-angled triangular, hexagonal and circular geometries were considered. Predicted C are given in fig. 4. With PV placed at one side only and external mirrors at the other sides, as shown in Fig 3, circular geometry obtains the highest C. For the range of A_{conc} considered, hexagonal geometry attains higher C than square or triangular, agreeing with experimental data in [10], and close to that obtained with the circular geometry. Practically, hexagonal geometry would allow more devices to be packed together, in a given space, than circular geometry would. With PV placed around all sides, predicted C are lower than those calculated for PV at one side only, as shown in Fig. 4. This is due to the increased A_{pv} and hence lower G_{geom}.

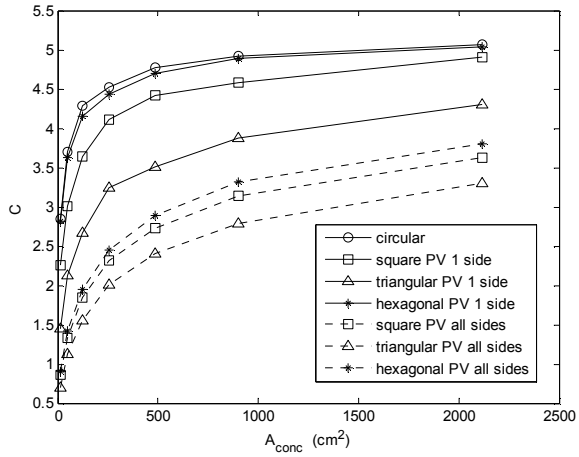

Fig. 4. Predicted concentration ratios (C).

3.2 2-D Geometry Relative Cost Per Unit Power

A larger C will result in a higher power output, indicating that hexagonal geometries might be the optimum. However, the cost of the concentrator plate (per m^2), although much lower than the cost of PV, is not negligible. Therefore, the geometry which attains the highest C is not necessarily the optimum. To determine the optimum geometry, the cost of the plate is factored in and the relative cost per unit power output is calculated, for each of the shapes and sizes considered in 3.1 excluding circular geometry. The results show that all geometries (whether PV is placed at one side only or around all sides) can attain approximately the same minimum cost per unit power.

For each particular shape and size, the relative power output is assumed to be proportional to the product of A_{pv} and the resulting C (eqn. 4). The relative total cost of a device is calculated using A_{conc} and A_{pv} (eqn. 5), where the variable *costfactor*, defining the cost of the concentrator plate per m^2 relative to the cost of PV, is given by eqn. 6. A costfactor of 20 is considered. Taking the cost of PV to be €600 per m^2, then the cost of the concentrator plate in this case would be €30 per m^2, similar to that estimated for a LSC plate containing a dye [11]. The relative cost per unit power output for each particular shape and size can then be calculated from eqn. 7.

$$\text{relative power} = (A_{pv}) \times C \quad (4)$$

$$\text{relative cost} = (A_{pv}) + \left(\frac{A_{conc}}{\text{costfactor}} \right) \quad (5)$$

$$\text{costfactor} = \frac{\text{cost of PV per m}^2}{\text{cost of concentrator plate per m}^2} \quad (6)$$

$$\text{relative cost per unit power} = \frac{\text{relative cost}}{\text{relative power}} \quad (7)$$

Fig 5 (a) and 5 (b) show the relative cost per unit power using a costfactor of 20. Hexagonal geometry, with PV attached to all sides, achieves the minimum cost per unit power. However, almost the same minimum (within 2%) is achieved for square geometry, indicating there would be no significant economic advantage in changing from the square geometry currently used in prototype QDSCs. Approximately the same minimum cost per unit power is achieved whether PV is placed at 1 side only, or at all sides.

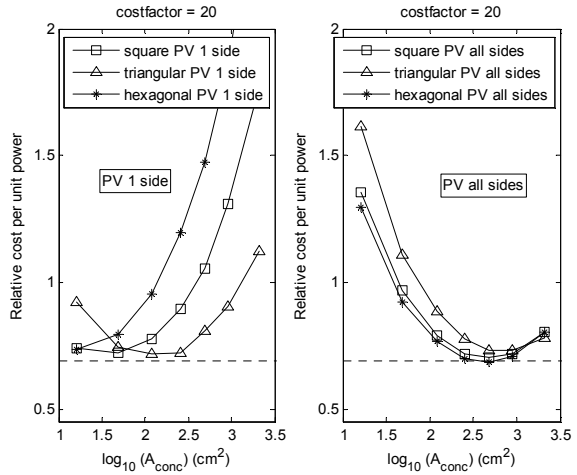

Fig. 5. Relative cost per unit power for different geometries. (a)-PV at one side only. (b)-PV at all sides. The price of concentrator plate per m^2 was assumed to be 20 times less than that of PV per m^2 (i.e. costfactor = 20).

It is noted that only the *number* of photons reaching the PV side has been considered here, and not the *spatial distribution* along the side. If PV cells are connected in series along one side, an uneven photon distribution will affect the overall electric current [12]. DeCardona et al. measured a more even distribution for polygons with higher numbers of sides indicating that hexagons will give the lowest cost per unit power.

3.3 3-D Geometry

Decreasing the thickness of the plate has two effects - G_{geom} increases, but η_{opt} decreases because less light is absorbed initially in the device. By increasing the QD concentration more light is absorbed, but there is more re-absorption and hence higher escape-cone losses. Using the range of QD concentrations shown in Fig. 2 and with PV attached to one side only, the peak C was calculated for square devices of varying uniform thickness. The top surface area (A_{conc}) remained constant at 121 cm^2. Fig. 6 (c) shows an increase in C with reduced thickness as was also shown in [6,10]. η_{opt} decreases with thinner plates but the increase in G_{geom} results in an overall increase in C for thinner plates.

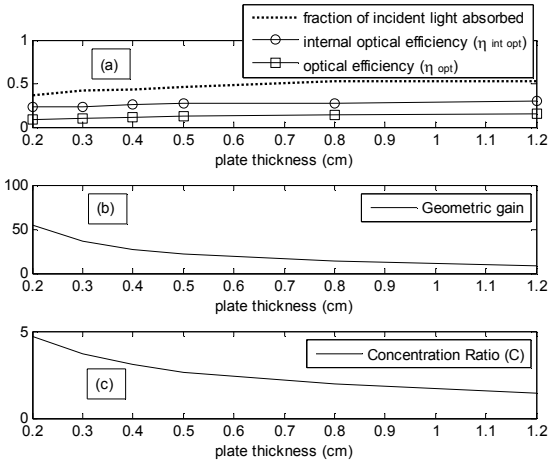

Fig. 6(a) shows a decrease in optical efficiency for thinner plates due to lower incident light absorption and internal optical efficiency. The increase in geometric gain (b), however, results in an increase in concentration ratio (c). A range of QD concentrations was used for each thickness.

Devices with tapered geometry, as shown in fig. 7, were also modelled. As the device is thicker on one side, it will allow more light to be absorbed than for a device with uniform thickness. This allows the possibility of a lower QD concentration being used, therefore reducing the re-absorption losses. The side where the PV is attached remains thin, maintaining a high G_{geom}. However, there is a decrease in η_{opt} due to the slope of the top and rear surfaces as some photons originally emitted inside the angular range for TIR are lost through the top surface, as illustrated in fig. 8. The model is used to determine if the combined effect is an increase or a decrease in C, compared to a device of uniform thickness. Using the range of QD concentrations shown in fig 2, C was calculated for varying side 2 thicknesses and varying side 1 lengths. The PV side thickness was kept constant at 0.3 cm. Devices with uniform thickness achieve the highest C as shown in fig. 9.

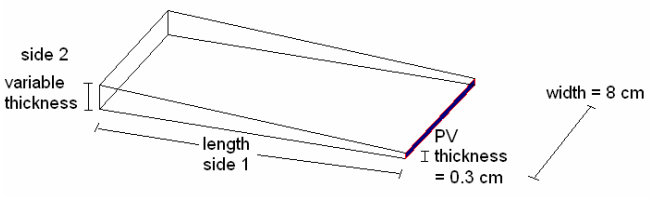

Fig. 7. Device with tapered geometry. The thickness of the PV side remains constant and the side 2 thickness and side 1 length are varied to investigate the effect on C.

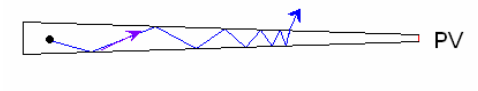

Fig 8. For tapered geometry, an emitted photon, originally inside the total internal reflection angular range, may be lost through the top due to the slope of the top and rear surfaces.

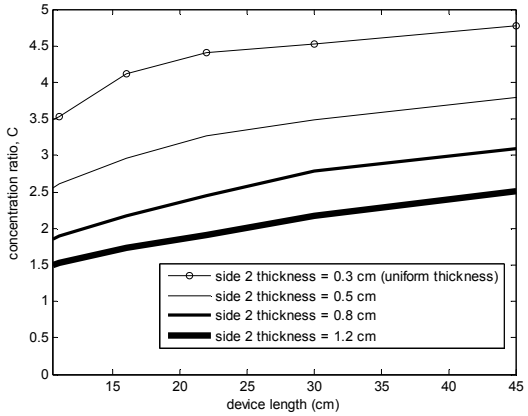

Fig. 9. Concentration ration (C) for device 0.3 cm thick (PV side) x 8 cm wide (see fig. 7). The thickness of side 2 and length of side 1 are varied. The highest C is obtained for devices of uniform thickness.

5. CONCLUSION

Using Monte-Carlo ray-trace modelling, concentration ratios (C) and the relative cost per unit power have been predicted for QDSCs of different 2-D geometries and sizes. Hexagonal geometry attains a higher C than square or triangular geometry, due to a higher G_{gain}. However, square geometry attains approximately the same minimum cost per unit power as hexagonal, when the cost of the concentrator plate is factored in. The same cost per unit power can be achieved whether PV is placed at one side or around all sides of the device. Hexagonal geometries do have a more uniform photon distribution along the PV side, which was not considered in the predicted C values. Hexagonal geometry would, therefore, have a lower cost per unit power than square or triangular. The relative cost analysis was not carried out for 3-d geometries, but it was found that C is lower for plates with tapered thickness than for plates of uniform thickness.

6. ACKNOWLEDGMENTS

The authors would like to acknowledge the collaboration of the EU-funded FULLSPECTRUM group, especially R. Koole of Utrecht University for supplying QD absorption and emission spectra. The Focas Institute is funded by the Irish Higher Education Authority with assistance from the European Regional Development Fund.

7. REFERENCES

(1) W. H. Weber, J. Lambe, “Luminescent greenhouse collector for solar radiation”, 1976, Applied Optics, 15, 2299-2300.
(2) A. Goetzberger, W. Greubel, “Solar Energy Conversion with Fluorescent Collectors”, 1977, Applied Physics, 14, 123-139.
(3) K.W. J. Barnham, J. L. Marques, J. Hassard, P. O'Brien, “Quantum dot concentrator and thermodynamic model for the global redshift”, 2000, Applied Physics Letters, 76, 9.
(4) S. J. Gallagher, B. Rowan, J. Doran, B. Norton, “Quantum dot solar concentrator: Device optimisation using spectroscopic techniques”, 2007, Solar Energy, 81, 4, 540-547.
(5) K. Heidler, A. Goetzberger, V. Witter, “Fluorescent Planar Concentrator. Monte-Carlo Computer Model, Limit Efficiency, and Latest Experimental Results”, 1982, Proceedings 4th EC PV Solar Energy Conference, Italy.
(6) M. Carrascosa, S. Unamuno, F. Agullo-Lopez, “Simulation of the performance of PMMA luminescent solar collectors”, 1983, Applied Optics, 22, 20, 3236-3241.
(7) S.J. Gallagher, P.C. Eames, B. Norton, “Quantum dot solar concentrator behaviour predicted using a ray trace approach”, 2004, International Journal of Ambient Energy, 25, 1, 47-56.
(8) A.R. Burgers, L.H. Sloof, R. Kinderman, J.A.M. Van Roosmalen, “Modelling of Luminescent Concentrators by Ray-tracing”, 2005, Proceedings of 20th European Photovoltaic Solar Energy Conference, Barcelona.
(9) M. Kennedy, B. Rowan, S. J. McCormack, J. Doran, B. Norton, “Modelling of a Quantum Dot Solar Concentrator and Comparison with Fabricated Devices”, 2007, Proceedings 3rd PV-SAT conference, Durham.
(10) J. Roncali, F. Garnier, “Photon-transport properties of luminescent solar concentrators: analysis and optimisation”, 1984, Applied Optics, 23, 16, 2809-2817.
(11) T. Meyer, Solaronix, 2007, Private communication.
(12) Sidrach De Cardona et al., “Edge effect on luminescent solar concentrators”, 1985, Solar Cells, 15, 225-230.